agronomy

MDPI

Article

Simulation of Staple Crop Yields for Determination of Regional Impacts of Climate Change: A Case Study in Chonnam Province, Republic of Korea

Jinsil Choi [1], Jonghan Ko [2,*], Kyu-Nam An [1], Saeed A. Qaisrani [3], Jong-Oh Ban [4] and Dong-Kwan Kim [1]

[1] Jeollanamdo Agricultural Research and Extension Services, Naju 58213, Korea; jinsil45@korea.kr (J.C.); ankyunam@korea.kr (K.-N.A.); kms1996@korea.kr (D.-K.K.)
[2] Aplied Plant Science, Chonnam National University, Gwangju 61186, Korea
[3] Environmental Sciences, COMSATS University, Islamabad 61100, Pakistan; saeed.qairani@cuivehari.edu.pk
[4] Management Information, Hallym Polytechnic University, Chuncheon-si 24210, Korea; banjo@hsc.ac.kr
* Correspondence: jonghan.ko@jnu.ac.kr; Tel.: +82-62-530-2053

Abstract: This study sought to simulate regional variation in staple crop yields in Chonnam Province, Republic of Korea (ROK), in future environments under climate change based on the calibration of crop models in the Decision Support System for Agricultural Technology Transfer 4.6 package. We reproduced multiple-year yield data for paddy rice (2013–2018), barley (2000–2018), and soybean (2004–2018) grown in experimental fields at Naju, Chonnam Province, using the CERES-Rice, CERES-Barley, and CROPGRO-Soybean models. A geospatial crop simulation modeling (GCSM) system developed using the crop models was then applied to simulate the regional impacts of climate change on the staple crops according to the Representative Concentration Pathway 4.5 and 8.5 scenarios. Simulated crop yields agreed with the corresponding measured crop yields, with root means square deviations of 0.31 ton ha^{-1} for paddy rice, 0.29 ton ha^{-1} for barley, and 0.27 ton ha^{-1} for soybean. We also demonstrated that the GCSM system could effectively simulate spatiotemporal variations in the impact of climate change on staple crop yield. The CERES and CROPGRO models seem to reproduce the effects of climate change on region-wide staple crop production in a monsoonal climate system. Added advancements of the GCSM system could facilitate interpretations of future food resource insecurity and establish a sustainable adaption strategy.

Keywords: climate change; crop model; region; simulation; staple crop; yield

Citation: Choi, J.; Ko, J.; An, K.-N.; Qaisrani, S.A.; Ban, J.-O.; Kim, D.-K. Simulation of Staple Crop Yields for Determination of Regional Impacts of Climate Change: A Case Study in Chonnam Province, Republic of Korea. *Agronomy* **2021**, *11*, 2544. https://doi.org/10.3390/agronomy11122544

Academic Editors: Ajit Govind, Chandrashekhar M. Biradar and Gniewko Niedbała

Received: 22 October 2021
Accepted: 13 December 2021
Published: 15 December 2021

1. Introduction

Increases in anthropogenic atmospheric greenhouse gases (GHGs) have led to an accompanying elevation in global mean surface temperatures of 0.74 °C ± 0.18 °C over the last 100 years (1906–2005), according to the Intergovernmental Panel on Climate Change (IPCC) [1]. The IPCC opined that the global warming trends from 1986–2005 to 2081–2100 would vary depending upon different GHG concentration trajectory scenarios. The IPCC report projects a temperature increase of 1.1 to 2.6 °C according to Representative Concentration Pathway (RCP) 4.5, and 2.6 to 4.8 °C based on RCP 8.5. It is also projected that elevated temperatures seemingly vary geographically and by region. Therefore, adaptative measures to climate changes that employ different strategies should be designed based on an adequate understanding of the socio-economic and local environments particular to each area.

The agricultural sector must produce sufficient food crops to meet the consumer demand of the future. However, the estimated increase in the concentrations of atmospheric GHGs and the combined elevation of temperature can impact crop production, which is mainly affected by changes in evapotranspiration, plant growth rates, plant litter composition, and the nitrogen-carbon cycle [2]. There have been various scientific endeavors

to measure global crop production, focusing on climate change [3–5]. It has been found that in some situations, global and regional crop productivity in a changing climate will fluctuate considerably due to the environmental variation among different regions [6–8], and the probable impacts in a particular area may differ depending on the extent of these fluctuations, as well as local crop responses, site-specific management, and socio-economic circumstances [9,10]. Therefore, it is essential to explore the local impacts of climate change on the production of crops of interest to enable the timely implementation of suitable adaptation measures for each region.

Crop morphogenesis, which is mainly influenced by genetic mechanisms and the combined effects of numerous eco-physiological processes within ecosystems, affects crop productivity variation. In addition, crop production is impacted by a number of ecosystem conditions (i.e., solar radiation, temperature, CO_2 concentration, soil nutrients and water) as well as field management. However, field experiments to evaluate the potential impacts of these physical characteristics on crop production have not been able to clarify all the environmental variables and their interactions. In this context, cropping system models that are adequately calibrated and validated can be used to examine the combined effects of chemical, physical, and biological processes [11,12]. Of a large number of crop models available, those frequently adopted for crop productivity assessments include the Agricultural Production System Simulator (APSIM) [13], the multidisciplinary simulator for standard crops (Stics) [14], the Root Zone Water Quality Model (RZWQM) [15], the Environmental Policy Integrated Climate (EPIC) [16], the World Food Studies (WOFOST) [17], and several crop models in the Decision Support System for Agrotechnology Transfer (DSSAT) package [18]. Agronomists and ecologists have generally used the crop models in the DSSAT package to investigate crop productivities under different environmental conditions and potential climate change scenarios. The DSSAT package, specifically version 4.7 (https://dssat.net, accessed on 1 October 2021), comprises crop models for over 42 crops, including the CERES models [19], CROPGRO [20], and SUBSTOR [21].

The IPCC scenarios project that regional variations will intensify in response to climate change [1]. In this regard, ROK is seemingly vulnerable to climate change, much in the same way or more than other regions. Therefore, it has been important for agricultural policymakers, scientists, and stakeholders in ROK to assess the impacts of climate change on crop productivity and create an appropriate crop plant for adaption. Different approaches have been developed to address the impacts of climate change, such as those derived from investigative field studies [22,23] and from studies using crop modeling practices [6,10]. Although recent crop modeling studies have attempted to project geographical variation in crop productivity as influenced by climate change impacts [24], little research has been conducted to investigate crop productivity variation at a regional scale in a changing climate in ROK [6,9]. Due to this country's complex topographical land characteristics, there are deeper field and inter-regional variations in crop productivity. Therefore, the objective of this study was to use a crop modeling approach to establish a scientific methodology to address the issue of local variations by projecting the geospatial variations in paddy rice, barley, and soybean yields in future environments under climate change in Chonnam Province, ROK. The study outcomes can be employed as a decision support tool to deliver the variation issue mentioned above.

2. Materials and Methods

2.1. Experimental Field Data for Rice, Barley, and Soybean

Field experiments were conducted at Jeollanamdo Agricultural Research and Extension Services (JARES; 35°1′ N, 126°45′ E; 14.7 m above sea level), Naju, Chonnam Province, ROK (Figure 1). The provincial inland region of Chonnam lies between the latitudes of 34°17′ and 35°29′ N and the longitudes of 126°5′ and 127°46′ E and has a total area of ~12,247 km^2. The 30-year average annual temperatures in this region, where barley (*Hordeum vulgare*), rice (*Oryza sativa*), and soybean (*Glycine max*) can be cultivated, range from ~12 to 15 °C, according to the Korea Meteorological Administra-

tion (KMA) (https://data.kma.go.kr/, accessed on 1 October 2021). The corresponding average annual total precipitation amounts vary from ~1200 to 1500 mm, of which ~60% of the rainfall is concentrated between June and September. Based on the United States Department of Agriculture classification system, the soil within the experimental area is classified as a Fluvisol with a loam texture with total organic carbon, total nitrogen, and available phosphate contents of 12.3 g kg^{-1}, 1.0 g kg^{-1}, and 13.1 g kg^{-1}, respectively, and a soil pH in H_2O of 5.5. Additional specific soil properties can be found in Yun et al. [25]. In addition, weather data were recorded using an automated weather station (WS-GP1; Delta-T Devices, Cambridge, UK).

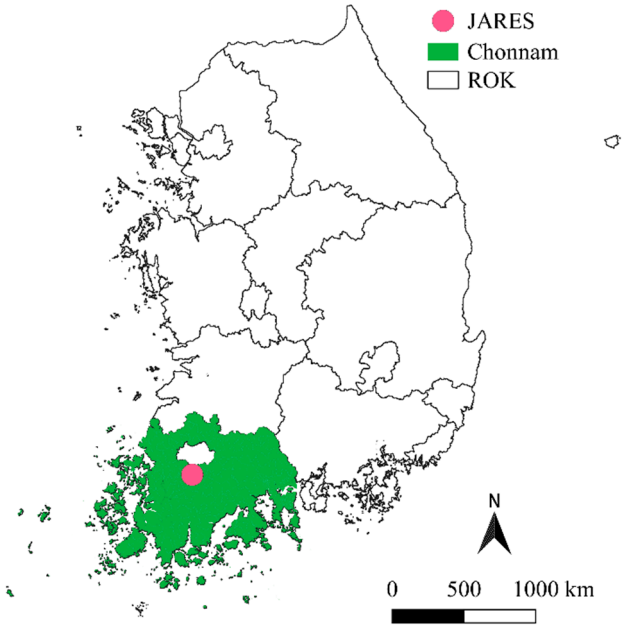

Figure 1. The study location map of Jeollanamdo Agricultural Research and Extension Services (JARES) and Chonnam Province, Republic of Korea (ROK).

The field experiments were carried out from 2000 to 2018 at JARES to simulate barley, rice, and soybean yields based on the determination of the genetic coefficients of each crop cultivar (Table 1). We deliberately selected six varieties of rice and barley and nine soybean varieties from among the available local crop cultivars bred by the National Institute of Crop Science (http://www.nics.go.kr/english/index.do, accessed on 1 September 2021). These crop cultivars were planted between the days of the year (DOY) 156 and 166 for rice, DOY 271 and 296 for barley, and DOY 164 and 176 for soybean in each crop field arranged as three randomized complete blocks with the planting densities of 27.3 hills m^{-2} for rice, 225 seeds m^{-2} for barley, and 22.2 seeds m^{-2} for soybean. During the 19 crop seasons, the areas were managed with optimum N–P_2O_5–K_2O fertilization of 80–70–35 kg ha^{-1} for barley, 90–45–57 kg ha^{-1} for rice, and 30–30–34 kg ha^{-1} for soybean. Paddy rice was grown using flood irrigation, while barley and soybean were fully irrigated with a sprinkler system. Crop yields were estimated by harvesting sample plants in each experimental plot from a 2 m^2 area for soybean and barley and 100 plants for rice. The plant samples for the yield estimation were harvested after physiological maturity at four replications in each crop field plot.

Table 1. Summary of crop cultivars, cultivation years, and planting dates and densities used in the study.

Crop	Cultivar and Cultivation Year	Planting Date in DOY [J]
Rice	Chopyong (2013–2015), Chonnam-3 (2013–2015), Ilmi (2016–2018), Nampyong (2016–2018), Saemnuri (2018), Hwangkeum (2016–2018)	DOY 156–166
Barley	Doosan 29 (2000–2018), Heenchal-naked (2012–2018), Hopum (2005–2018), Jinyang (2000–2018), Saechal (2000–2018), Saechal-naked (2000–2018)	DOY 271–296
Soybean	Daewon (2011–2018), Daweon (2006–2014), Daepung (2013–2014), Haepoom (2014–2018), Pungsannamul (2003–2018), Pungwon (2011–2014), SeoNam (2003–2005, 2008–2010), SoWeon (2003–2006), Tawkwang (2011–2018)	DOY 161–176

[J] DOY represents day of the year.

2.2. Crop Models

Crop models are conceptually designed to simulate productivity in relation to environmental and biophysical factors (Figure A1). Of the crop models available for the crop production simulation, we employed CERES-Rice, CERES-Barley, and CROPGRO-Soybean from the DSSAT package [15] to simulate the impacts of climate change on rice, barley, and soybean, respectively, in Chonnam Province, ROK. The DSSAT crop models are process-based management-level simulation models developed to reproduce field conditions of crop morphogenesis, crop yield, soil water, and soil nutrient balance associated with crop growth. In this study, we used the CERES-rice, CERES-barley, and CROPGRO-soybean models differently to simulate all the cultivars (Table 1) from common practice. We used the Genotype Coefficient Calculator tool in the DSSAT package to determine the generic coefficients of each cultivar. We also manually calibrated the coefficients proposed by Goodin et al. [26]. The parameter values determined for each cultivar are presented in Tables 2–4. In the CERES and CROPGRO models, climate, CO_2 concentration, and soil data are independent variables. However, it appears that the long-term global environment depends on global greenhouse gases, including CO_2 concentration. Therefore, it seems that CO_2 concentration can affect crop growth via changes in temperature and solar radiation. The crop models determine the net biomass production using the radiation use efficiency (RUE) approach. Impacts of elevated CO_2 concentration on RUE were formulated empirically using curvilinear multipliers [27]. The empirical formula uses a y-intercept in a modified Michaelis–Menten equation to fit crop responses to a range of CO_2 concentrations:

$$R = \frac{R_m \cdot CO_2}{CO_2 + K_m} + R_i \quad (1)$$

where R is RUE, as linked to yield or other responses; R_m is the asymptotic response limit of $(R - R_i)$ at a high CO_2 concentration; R_i is the intercept on the y-axis; and K_m is the value of the substrate concentration (i.e., CO_2), at which $(R - R_i) = 0.5\ R_m$. Analogous methodologies have been adopted to simulate the effect of CO_2 on cropping systems in EPIC [13], Agricultural Production Systems Simulator [28], and Sirius [29].

Table 2. Genetic coefficients of six rice cultivars.

Coeff. †	Default ‡	Ilmi	Nampyeong	Saenuri	Hwangkeum	Chopyong	Chonnam-3
P1	220.0	320.0	300.0	200.0	400.0	320.0	390.0
P2O	12.0	12.8	12.8	12.8	12.8	12.8	12.8
P2R	35.0	20.0	90.0	10.0	45.0	35.0	20.0
P5	510.0	530.0	550.0	530.0	670.0	500.0	530.0
G1	55.0	65.0	65.0	65.0	65.0	65.0	65.0
G2	0.025	0.022	0.022	0.021	0.024	0.021	0.021
G3	1.0	1.2	1.2	1.3	1.2	1.2	1.2
G4	1.0	1.0	1.0	1.0	1.0	1.0	1.0

† P1, Time period (expressed as growing degree days [GDD] in °C above a base temperature of 9 °C) from seedling emergence during which the rice plant is not responsive to changes in photoperiod; P2O, Critical photoperiod or the longest day length (in hours) at which the development occurs at a maximum rate; P2R, Extent to which phasic development leading to panicle initiation is delayed (expressed as GDD in °C) for each hour increase in photoperiod above P20; P5, Time period (expressed as GDD in °C) from the beginning of grain filling (three to four days after flowering) to physiological maturity with a base temperature of 9 °C; G1, Potential spikelet number coefficient as estimated from the number of spikelets per g of main culm dry weight (less lead blades and sheaths plus spikes) at anthesis; G2, Single grain weight (g) under ideal growing conditions, that is, non-limiting light, water, nutrients, and absence of pests and diseases; G3, Tillering coefficient (scaler value) relative to IR64 cultivar under ideal conditions; and G4, Temperature tolerance coefficient. ‡ Default values are from the Japanese cultivar in CERES-Rice version 4.6.

Table 3. Genetic coefficients of four barley cultivars.

Generic Coefficient †	Default ‡	SaeChal	SaeChal-Naked	Doosan 29	Jinyang	Hopum	HeenChal-Naked
P1V	5	10	10	10	10	10	10
P1D	75	23	23	20	20	20	20
P5	450	200	200	180	180	200	100
G1	30	22	22	22	20	22	22
G2	35	55	49	35	40	35	45
G3	1.0	1.5	1.5	1.5	1.5	1.5	1.5
PHINT	60	90	90	93	83	80	80

† P1V, Optimum temperature required for vernalization (day); P1D, Photoperiod response (% reduction in the rate per 10 h drop in the photoperiod); P5, Grain filling (excluding lag) phase duration (°C day); G1, Kernel number per unit canopy weight at anthesis; G2, Standard kernel size under optimum conditions (mg); G3, Standard non-stressed mature tiller weight (g); and PHINT, Interval between successive leaf tip appearances (°C day). ‡ Default values are from the Default cultivar in CROPGRO-Soybean version 4.6.

Table 4. Genetic coefficients of seven soybean cultivars.

Coeff. †	Default ‡	Daewon	Taekwang	Pungsan	Haepoom	Daepung	Pungwon	Dawon
CSDL	14.60	14.80	14.61	13.92	13.58	12.04	12.57	12.02
PPSEN	0.129	0.345	0.32	0.344	0.287	0.266	0.249	0.241
EM-FL	15.5	21.0	21.0	22.5	19.2	18.0	18.0	16.5
FL-SH	5.0	6.0	6.0	6.0	9.0	8.0	9.0	9.0
FL-SD	12.0	13.0	13.0	12.0	13.0	14.0	16.0	16.0
SD-PM	29.5	34.5	34.0	34.0	35.5	32.0	32.0	32.6
FL-LF	26.0	18.0	18.0	18.0	18.0	26.0	26.0	26.0
LFMAX	1.03	1.03	1.03	1.03	1.03	1.03	1.02	1.02
SLAVR	375	375	375	400	375	385	375	390
SIZLF	180	180	180	150	180	180	170	180
WTPSD	0.19	0.19	0.19	0.19	0.15	0.19	0.18	0.17
SFPDV	23.0	23.0	22.0	24.0	23.0	21.0	21.0	22.0

† CSDL, Critical short day length below which reproductive development progresses with no day-length effect for short-day plants (hour); PPSEN, Slope of the relative response of development to photoperiod with time (positive for short day plants) (1/hour); EM-FL, Time between plant emergence and flower appearance (R1) (photo-thermal days); FL-SH, Time between first flower and first pod (R3) (photo-thermal days); FL-SD, Time between first flower and first seed (R5) (photo-thermal days); SD-PM, Time between first seed (R5) and physiological maturity (R7) (photo-thermal days); FL-LF, Time between first flower (R1) and end of leaf expansion (photo-thermal days); LFMAX, Maximum leaf photosynthesis rate at 30 °C, 350 vpm CO_2, and high light (mg CO_2/m^2s^{-1}); SLAVR, Specific leaf area of cultivar under standard growth conditions (cm^2/g); SIZLF, Maximum size of full leaf (three leaflets) (cm^2); WTPSD, Maximum weight per seed (g); and SFPDV, Average seed per pod under standard growing conditions (#/pod). ‡ Default values are the M Group 000 cultivar from in CROPGRO-Soybean version 4.6.

The minimum variables for driving model simulations are daily solar radiation, maximum and minimum temperatures, and precipitation. In addition, the required parameters include crop genetic coefficients, physical and hydraulic soil characteristics, initial soil nitrogen and soil water conditions, and typical crop management metadata (i.e., the planting date, planting depth, plant population density, and the amounts and methods of irrigation and fertilizer applications). There are eight genetic coefficients in CERES-rice, seven in CERES-barley, and twelve in CROPGRO-soybean (Tables 2–4). The three models characterize the growth process of the related crop species using these genetic coefficients.

2.3. Geospatial Simulation of the Climate Change Impacts

The geospatial crop simulation modeling (GCSM) scheme was formulated using each of the CERES-rice, CERES-barley, and CROPGRO-soybean crop models. In the present study, the GCSM system used previously [6,30] was further developed to simulate the potential impacts of climate change on regional projections of rice, barley, and soybean yields. Using shell scripting in the Linux operating system, the GCSM scheme was designed to run the crop models as many times as planned using pixel-based two-dimensional climate and soil data (Figure 2). We also designed that model so that input parameter conditions of interest could be manipulated in the GCSM, including cultivar selection, planting date, planting density, soil fertilization, and environmental modification options (i.e., temperature, solar radiation, and CO_2 concentration). The GCSM strategy allows the whole geographical region to be divided into a two-dimensional array of pixels, with each pixel representing an area of 1 km × 1 km. The pixel-by-pixel soil data provided by the National Academy of Agricultural Science (NAAS), ROK (http://soil.rda.go.kr/eng/, accessed on 1 September 2021), and the projected climate data provided by the KMA were preprocessed and used as input for the crop models to generate pixel-by-pixel projected crop yield values for the next 100 years. We predetermined the eight probable soil input archives for crop cultivation in Chonnam Province from the combined soil information using the generic soil input list of the DSSAT package (Table A1). A detailed soil inventory can be accessed in Hong et al. [31].

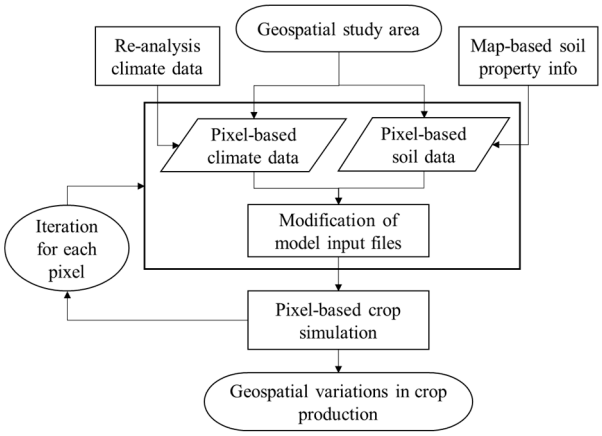

Figure 2. Geospatial crop simulation modeling scheme.

2.4. Data for the Crop Simulation

The CERES-rice, CERES-barley, and CROPGRO-soybean models were calibrated and validated using the rice, barley, and soybean datasets, respectively; these were obtained from the JARES experimental fields (Table 1). Thereafter, the models in the GCSM were applied to simulate the future impacts of climate change on these crops for the whole geographical region of Chonnam Province, ROK.

The environmental data applied to simulate the impact of climate change on rice, barley, and soybean yields in this study included: (1) soil data, (2) projected climate data, and (3) projected CO_2 concentration data. We obtained grid-based pixel soil data from

digital soil maps (1:5000) for the entire Chonnam Province provided by the NAAS. These soil data were used to aggregate information about topsoil properties, soil type, adequate soil depth, and soil structure for the region to determine soil input parameters of the crop models in the GCSM system. The GCSM system was designed to analytically select one of the eight prospective soil input libraries, preset for crop cultivation in Chonnam Province, based on the combined soil information using the generic soil input inventory of the DSSAT package v4.6). We used Chonnam Province climate data from 12 years (1999–2011) with a 1 km ground resolution as a baseline for the crop model input in the GCSM regime. These grid-based climate data were obtained utilizing a dynamic downscaling method to determine high-resolution regional agro-climate indices using a regional climate model, namely, the Weather Research and Forecasting Model [32].

2.5. Climate Projections

The regional climate model, HadGEM3-RA, and the general circulation model, HadGEM2-AO, were used to simulate regional climate change projections for Chonnam Province under two GHG concentration trajectory scenarios, i.e., RCP 4.5 and RCP 8.5 [1]. The prediction of climate variables included temperature and precipitation. We obtained climate change scenarios from the Coordinated Regional climate Downscaling Experiment (CORDEX) initiative produced by the Task Force for Regional Climate Downscaling and created by the World Climate Research Programme in 2009. Large-scale climate variables from HadGEM2-AO were dynamically downscaled to a physically consistent evolution on a lesser scale (0.44 × 0.44°) scale using the HadGEM3-RA model. Additional information on these climate models can be found on the CORDEX-East Asia website (http://cordex-ea.climate.go.kr/, accessed on 1 September 2021). Chonnam Province temperature and precipitation changes associated with CO_2 concentrations under the RCP4.5 and RCP8.5 scenarios were simulated for future years, particularly 2044–2056 centered on 2050, 2064–2076 centered on 2070, and 2094–2106 centered on 2100. Regional shifts estimated from the baseline regional climate data were integrated into the primary climate change trend to produce regional projections of daily climate data (Table 5). We used these projected data to comprise interannual climate changeability. These variations in temperature and precipitation were superimposed on the 12-year baseline. This approach was formerly used to estimate daily climate change in the Central Great Plains, USA [33], and for the whole topographical region of ROK [6].

Table 5. Projections of temperature (T) and precipitation (P) changes associated with the elevated CO_2 concentrations according to the Representative Concentration Pathway (RCP) scenarios.

RCP Scenario	Year	CO_2 (ppm)	T Change (°C)	P Change (%)
4.5	2050	480	+0.9	+3
	2070	520	+1.9	+6
	2100	540	+2.3	+7
8.5	2050	530	+1.5	+3
	2070	680	+2.7	+7
	2100	940	+4.3	+10

2.6. Statistical Analysis

We used four statistical agreement criteria to assess the model performance of the simulation of yield. These criteria were the *p*-value from a paired *t*-test; mean absolute error (MAE), Equation (2); root means square deviation (RMSD), Equation (3); and Nash-Sutcliffe model efficiency (*NSE*) [34], Equation (4).

$$MAE = \frac{\sum_{i=1}^{n} |S_i - M_i|}{n} \quad (2)$$

$$RMSD = [\frac{1}{n}\sum_{i=1}^{n}(S_i - M_i)^2]^{1/2} \quad (3)$$

$$NSE = 1 - \frac{\sum_{i=1}^{n}(S_i - M_i)^2}{\sum_{i=1}^{n}(M_i - M_{avg})^2} \quad (4)$$

where n is the number of data pairs and S_i, M_i, and M_{avg} represent ith simulated, ith measured, and mean measured values, respectively. The *NSE* determines how well the plot of the measured data compared to the simulated data resembles the 1:1 line. The *NSE* values change from $-\infty$ to 1. The nearer the value is to one, the more precise the model is. The smaller or closer it is to zero, the lower the model estimate accuracy is.

3. Results

3.1. Simulation of Rice, Barley, and Soybean Yields

The CERES-rice, CERES-barley, and CROPGRO-soybean models reproduced field variations in rice, barley, and soybean yields for multiple years and different cultivars (data not shown) with a significant agreement (Figures 3 and A2, and Table 6). The simulated rice yields agreed with the measured rice yields with a *p*-value of 0.66 according to a two-sample *t*-test, an RMSD of 0.209 ton ha^{-1}, and an NSE of 0.96 in model calibration, having a *p*-value of 0.99 according to a two-sample *t*-test, an RMSE of 0.455 ton ha^{-1}, and an NSE of 0.24 in model validation. Simulated soybean yields agreed with the measured soybean yields with a *p*-value of 0.80 according to a two-sample *t*-test, an RMSD of 0.141 ton ha^{-1}, and an NSE of 0.97 in model calibration, having a *p*-value of 0.51 according to a two-sample *t*-test, an RMSE of 0.424 ton ha^{-1}, and an NSE of 0.81 in model validation. Simulated barley yields agreed with the measured barley yields with a *p*-value of 0.69 according to a two-sample *t*-test, an RMSD of 0.132 ton ha^{-1}, an NSE of 0.94 in model calibration, having a *p*-value of 0.48 according to a two-sample *t*-test, an RMSE of 0.453 ton ha^{-1}, and an NSE of 0.60 in model validation. Together, the crop models could reproduce the yields of rice, soybean, and barley with *p*-values of 0.64, 0.62, and 0.42, respectively, according to two-sample *t*-tests, having RMSD values of 30.6, 27.0, and 29.3 ton ha^{-1} and NSE values of 0.89, 0.94, and 0.77, respectively.

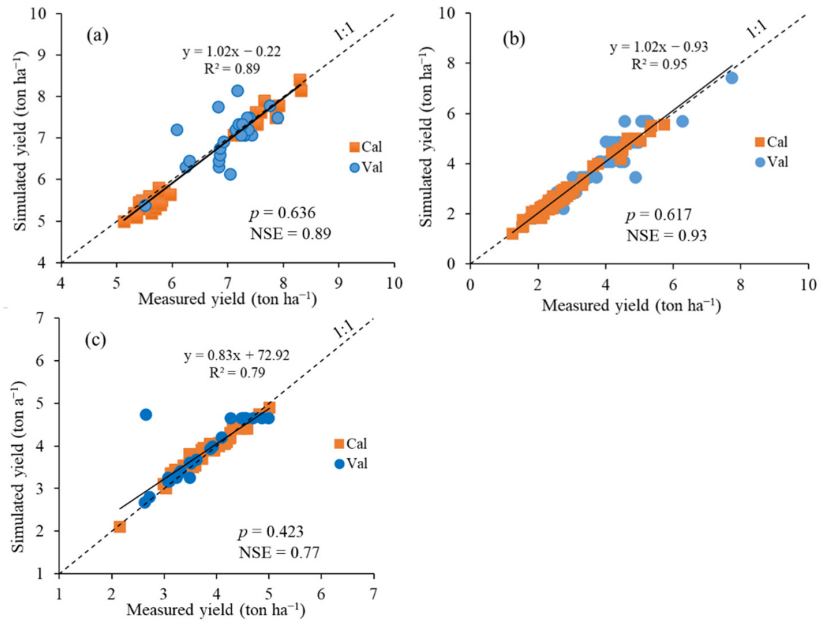

Figure 3. Simulated versus measured paddy rice (**a**), soybean (**b**), and barley (**c**) yields in calibration (Cal) and validation (Val). *p*, *n*, and NSE represent *p*-values in two-sample *t*-tests, data points, and Nash-Sutcliffe model efficiency, respectively.

Table 6. Statistical indices of mean absolute error (MAE), root mean squared deviation (RMSD), two-sample *t*-test (*p*), and Nash-Sutcliffe model efficiency (NSE) of the simulated (Sim) and measured (Meas) rice, soybean, and barley yields in calibration (Cal) and validation (Val).

Crop	Evaluation	Sim	Meas	MAE	RMSD	*p* (a = 0.05)	NSE
		ton ha^{-1}					
Rice	Val (2017–18)	7.00 ± 0.615	7.00 ± 0.535	0.319	0.455	0.99	0.24
	Cal (2013–16)	6.29 ± 1.712	6.41 ± 1.071	0.171	0.209	0.66	0.96
Soybean	Val (2014–18)	4.12 ± 1.034	4.00 ± 0.974	0.312	0.424	0.51	0.81
	Cal (2003–13)	2.69 ± 0.868	2.66 ± 0.846	0.126	0.141	0.80	0.97
Barley	Val (2010–18)	3.89 ± 0.697	3.75 ± 0.729	0.213	0.453	0.48	0.60
	Cal (2000–09)	3.85 ± 0.502	3.81 ± 0.552	0.112	0.132	0.69	0.94

As CO_2 concentration increases, rice, soybean, and barley yields are projected to increase up to a plateau of about 400 ppm (Figure 4). Conversely, rice yield decreases as temperature elevates, soybean yield generally maintains constant, showing a bit of fluctuation, and barley yield increases until 2.5 °C. The combined effects of temperature and CO_2 on these crop yields show a slow decline in rice, a plateau in soybean, and an increase until 2.5 °C in barley, and the same for the temperature responses.

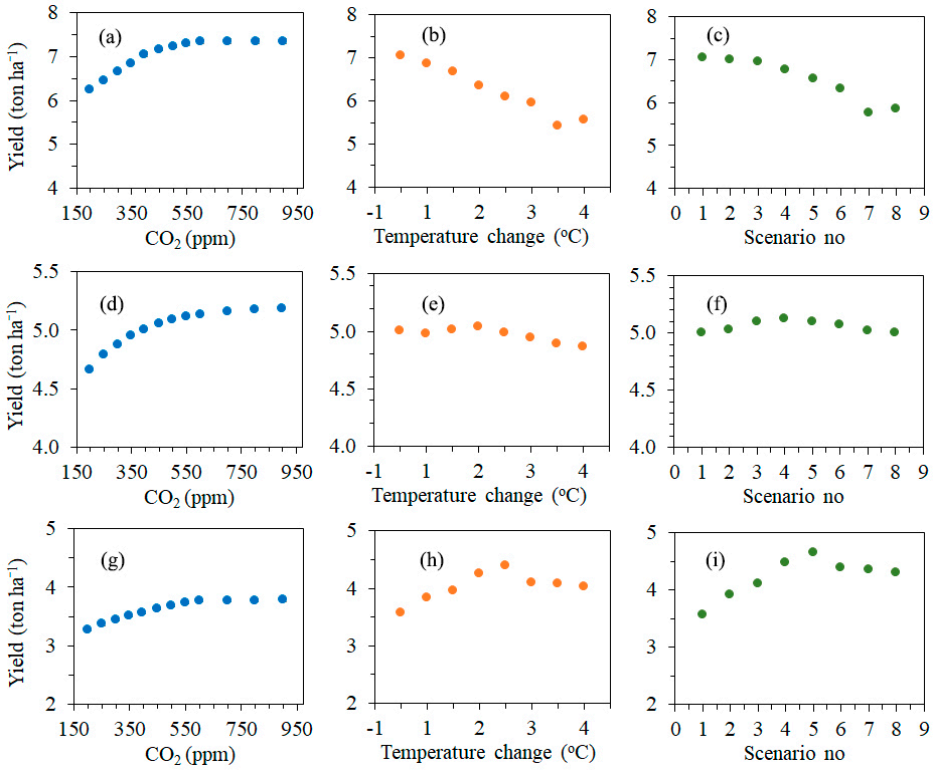

Figure 4. Simulated yield responses of rice (**a**–**c**), soybean (**d**–**e**), and barley (**g**–**i**) to the climate change factors of CO_2, temperature, and combined scenrios of tmeperature (T) and CO_2 (C) (1 = baseline, 2 = T0.5 °C + C450 ppm, 3 = T1.0 °C + C500 ppm, 4 = T1.5 °C + C550 ppm, 5 = T2.0 °C + C600 ppm, 6 = T2.5 °C + C700 ppm, 7 = T3.0 °C + C800 ppm, and 8 = T3.5 °C + C900 ppm).

3.2. Geographical Simulation of the Climate Change Impacts

We employed the CERES-rice, CERES-barley, and CROPGRO-soybean models in the GSCM system to simulate the potential influences of climate change on rice, barley, and soybean yields in the whole geographical area of Chonnam Province, ROK. As a result, these crop yields were projected for the target years 2050, 2070, and 2100 with the RCP 4.5 and RCP 8.5 scenarios. According to the RCP 4.5 scenario, Ilmi rice yields decreased by 4.0% and 6.9% in 2050 and 2070, respectively, showing a 1.3% increase in 2100 (Figure 5). In contrast, Daewon soybean yields showed small increases at 4.0%, 3.5%, and 3.9% in 2050, 2070, and 2100, whereas SaeChal-naked barley yields increased 20.8%, 26.3%, and 17.5% in 2050, 2070, and 2100, respectively (Figures 6 and 7). Regarding the RCP 8.5 scenario, rice and soybean yields were projected to increase slightly compared to the baseline, whereas barley yields were projected to increase gradually (Figures A3–A5). However, we found that the crop yields under RCP 8.5 fluctuated more than those under the RCP 4.5 during the projected years. Furthermore, we found that the barley yields showed the highest geospatial variation, with values between ±20.9% and 30.9% of the mean values, followed by the rice yields. We also found that crop yields were projected to be comparatively higher in the coastal areas of Chonnam Province but lower in the interior mountainous regions.

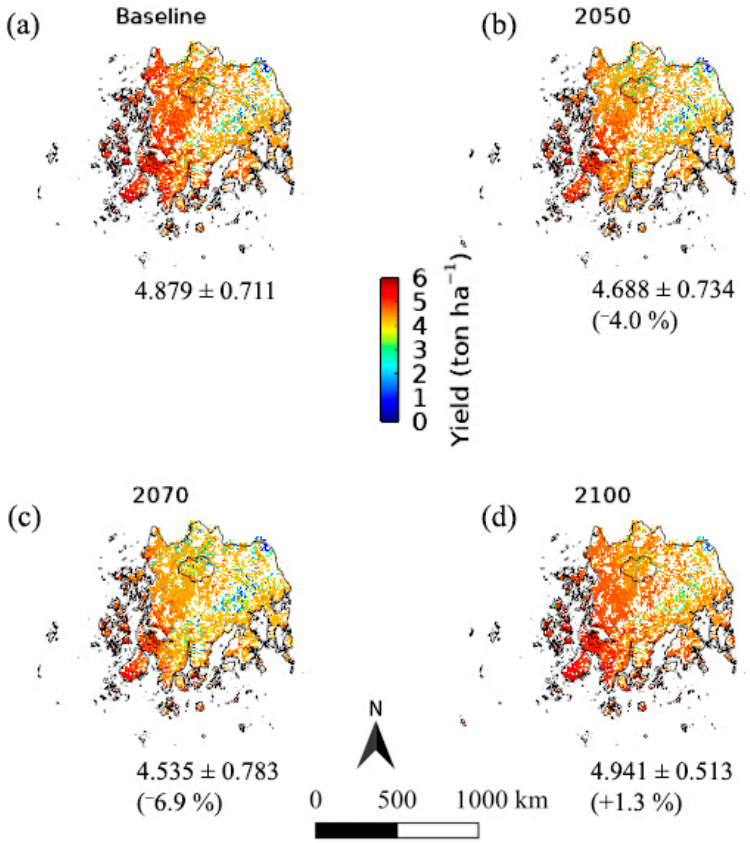

Figure 5. Simulated variations in Ilmi rice yield under the potential climate change impacts of Representative Concentration Pathway (RCP) 4.5 in 2044–2056 centered on 2050 (**b**), 2064–2076 centered on 2070 (**c**), and 2094–2106 centered on 2100 (**d**) compared to the baseline (**a**) in Chonnam Province, Korea. The values in the parentheses represent the yield change percentages in comparison with the baseline yield.

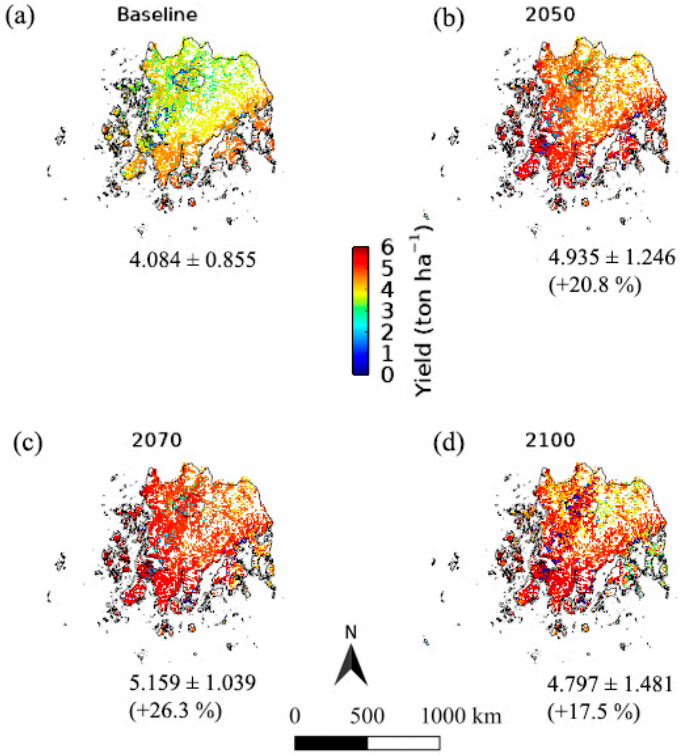

Figure 6. Simulated variations in SaeChal-naked barley yield under the potential climate change impacts of RCP 4.5 in 2044–2056 centered on 2050 (**b**), 2064–2076 centered on 2070 (**c**), and 2094–2106 centered on 2100 (**d**) compared to the baseline (**a**) in Chonnam Province, Korea. The values in the parentheses represent the yield change percentages in comparison with the baseline yield.

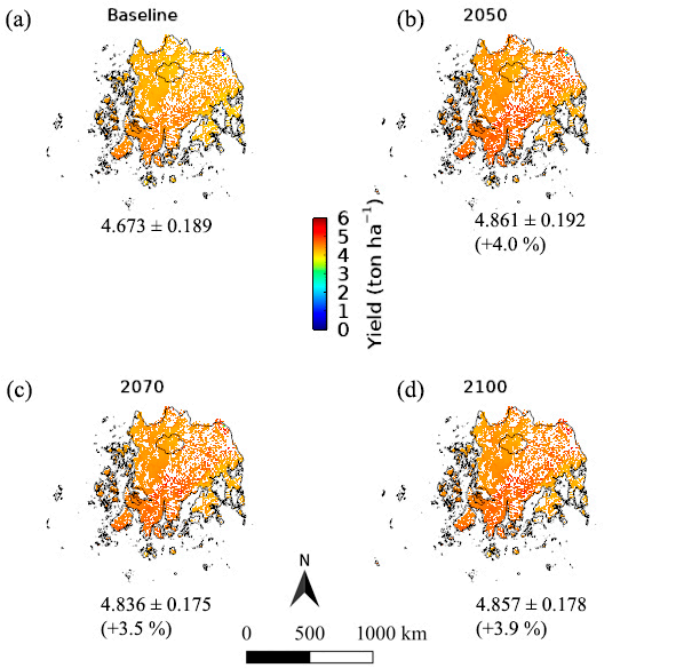

Figure 7. Simulated variations in Daewon soybean yield under the potential climate change impacts of RCP 4.5 in 2044–2056 centered on 2050 (**b**), 2064–2076 centered on 2070 (**c**), and 2094–2106 centered on 2100 (**d**) compared to the baseline (**a**) in Chonnam Province, Korea. The values in the parentheses represent the yield change percentages in comparison with the baseline yield.

4. Discussion

In this study, we successfully calibrated and validated CERES-rice, CERES-barley, and CROPGRO-soybean models for yield simulations of rice, barley, and soybean grown in the JARES fields, following which we reproduced the geographical variation in crop yield in the Chonnam region of South Kore. Based on earlier reports, we surmised that these crop models could be employed to simulate climate change impacts on the yields of these crops. A recent study demonstrated this capability by reproducing barley and paddy rice productions under the temperature gradient chamber system in the region of interest using the CERES-barley and CERES-rice models [6,10]. In addition, it was previously reported that models could simulate the CO_2 effects of a free-air CO_2 enrichment system on the productivity of the crop of interest [35–37]. However, although these models provided successful outcomes for these studies, they need to be further developed to address more sophisticated issues and important future field crop research. For example, the improvement could include but is not limited to detailed modeling of crop development and growth performance, as well as plant-water-soil-nutrient interactions.

The current study further utilized a previously developed GCSM system [6,30] to simulate the potential impacts of climate change on regional projections of rice, barley, and soybean yields. As a result, we adequately represented spatial variations in these crop yields within geographical regions of the whole of Chonnam Province, showing higher yields in the coastal areas and lower yields in the inner mountainous regions. Although there have been sufficient research endeavors to compute global crop production, particularly considering the influences of climate change [38,39], it is not possible at present to measure the collective impact of climate change on global agricultural productivity [40]. These complexities are mainly attributable to difficulties in classifying appropriate cultivated lands, insecurities in climate projection models, as well as genetic, environmental, and regional inconsistencies in crop production. Furthermore, the global land distribution suitable for growing crops is prone to continuous change resulting from the current driving forces of environmental fluctuations, socio-economic development, and the potential impacts of climate change [5]. Therefore, it is also probable that the unpredictability in regional and global crop productivity will substantially change over time [7,41]. There has been some effort elsewhere to reproduce geospatial variations in the effects of climate change on staple crops, such as paddy rice in Southeast Asia [42] and maize and beans in East Africa [43]. However, it is necessary to design a two-dimensional crop modeling system to project spatiotemporal crop productivity at a fine grid scale to determine local variations in crop production. To the best of our knowledge, the present study is the first in which the effects of climate change on rice, barley, and soybean have been simulated using a fine grid (1 km)-based local yield projection.

Future fluctuations in temperature and precipitation could create crop water demands and declines in yields; however, elevated CO_2 levels have improved crop yields in US agriculture [33,44,45]. Yield declines could negate CO_2 fertilization effects on crops due to the increase in temperature, which could be mitigated by appropriate cultivar selection and a reasonable planting time. Hence, this finding indicates that temperature changes could either positively or negatively affect crop productivity depending on the cultivar selection, as evidenced by the effects of temperature on crop yields in the Chonnam region (see Figures 4–7). It appears that temperature effects on a crop cultivar could dominate the impacts of other climate factors. Therefore, various cultivation options, including planting and cultivar alternatives, might be measures to overcome the potential impacts of climate change on crop production in future years.

Previously, the CERES-rice model was applied to project the potential impacts of climate change on paddy production for other short-grain rice-producing regions in East Asia [10]. This model was also employed to simulate the effects of climate change on rice yield at different altitudes in mountainous landscapes [9]. The study findings indicated that temperature effects in the lower latitudinal areas would dominate the impact. For the latitudinal range of approximately 34° to 42°, CO_2 fertilization would negate

any unfavorable consequences of temperature. The current study results are consistent with this finding, which we projected to be somewhat similar for the rice and soybean yields in Chonnam Province (see Figures 3, 5, A3 and A5). For crops grown at higher latitudes (i.e., >42°), positive effects on yield would be primarily attributable to the effect of temperature with minor impacts of CO_2 fertilization. Thus, the combined effects of CO_2, temperature, precipitation and solar radiation on crop yields in diverse latitudinal regions were mainly attributed to CO_2 and temperature [10,45]. Whereas these study results demonstrated a general resemblance to those presented by Adams et al. [44] and Hatfield et al. [46], conveying that different climate change projections with maximum and minimum temperature variability in various regions might show different results. This matter supports the current study effort and further investigations, which are essential to address the accompanying issues of food insecurity. However, a limitation of the present study is that the regional projection results are likely biased as the climate projection model employed depended on the regional down-scaled ensemble model based on the single general circulation model projection.

5. Conclusions

This research demonstrated that the CERES-rice, CERES-barley, and CROPGRO-soybean models could be utilized at a local scale to investigate the effects of climate change on rice, barley, and soybean production under the climate of Chonnam Province, ROK. We found that the future productivity of rice, barley, and soybean in the Chonnam region is likely to be dominated by the temperature elevation, counterbalancing the effects of CO_2 fertilization. Furthermore, the developed GCSM system using the CERES and CROPGRO models in the DSSAT package could simulate geospatial variations in crop productivity under different climate change scenarios. A strength of the study is that the regional topographical productivity variation issue can be delivered using the developed GCSM system based on the well-evaluated crop model. Although the GCSM system formulated in this study needs additional adjustment to meet requirements as an independent tool for scientists and stakeholders, we believe that this system could be effectively applied to simulate geographical variations of the impacts of climate change on staple crops. This well-formulated system can eventually be utilized as a decision support tool to address the geographical productivity variation issue. In addition, this technique could also be employed to explore feasible clarifications for easing the insecurity surrounding food safety measures.

Author Contributions: J.K. and J.C. designed the research and wrote the first draft; K.-N.A. and D.-K.K. obtained the data; J.C. and S.A.Q. analyzed the data; J.K. and J.-O.B. developed the modeling system; and all authors contributed to organizing the final draft. All authors have read and agreed to the published version of the manuscript.

Funding: This research was supported by Chonnam National University, Gwangju, and the Cooperative Research Program for Agriculture Science & Technology Development (Pro-ject No. PJ01010702) from the Rural Development Administration, Republic of Korea. In addition, partial financial assistance was provided from the Basic Science Research Program through the National Research Foundation of Korea (NRF-2021R1A2C2004459).

Institutional Review Board Statement: Not applicable.

Informed Consent Statement: Not applicable.

Acknowledgments: The authors would like to thank Mark Murdaugh for English language editing.

Conflicts of Interest: The authors declare that there is no conflict of interest.

Appendix A

Table A1. Soil information summary for the generic soil input inventory of the Decision Support System for Agrotechnology Transfer (DSSAT) package v4.6 used in this study.

ID	Texture	Depth (cm)	Soil Water † (cm^3 cm^{-3})	
			CLL	DUL
IB00000002	Medium silty clay	150	0.228	0.385
IB00000003	Shallow silty clay	60	0.228	0.385
IB00000005	Medium silty loam	150	0.108	0.218
IB00000006	Shallow silty loam	60	0.108	0.218
IB00000008	Medium sandy loam	150	0.052	0.176
IB00000009	Shallow sandy loam	60	0.052	0.176
IB00000011	Medium sand	150	0.024	0.096
IB00000012	Shallow sand	60	0.024	0.096

† Volumetric water content of the topsoil averaged among 5, 15, and 30 cm at the crop lower limit (CLL) and at the drained upper limit (DUL).

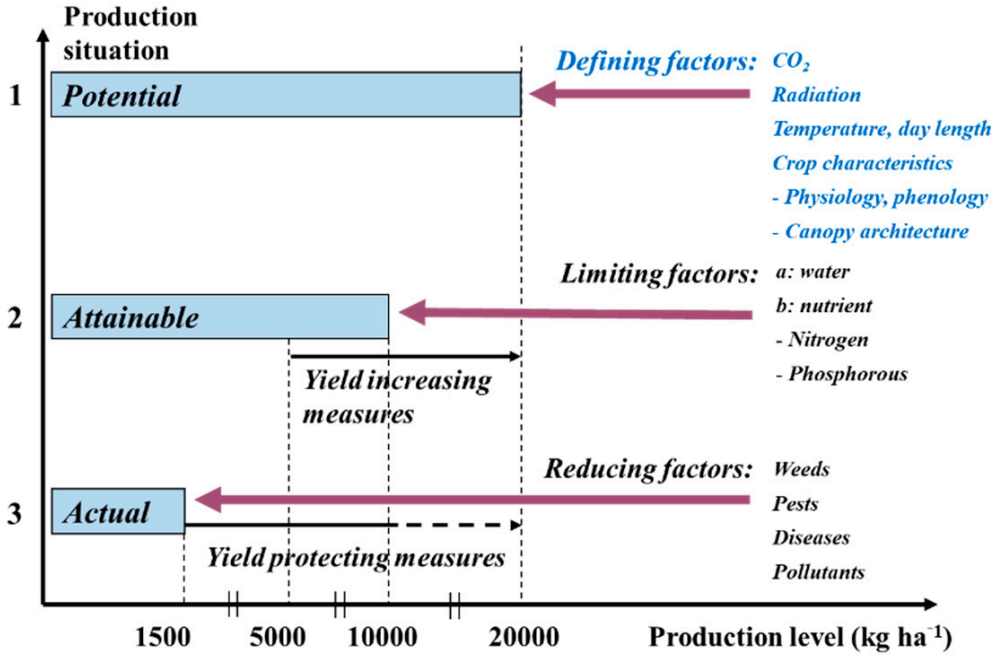

Figure A1. Crop model concepts (modified from Lövenstein et al. [47]).

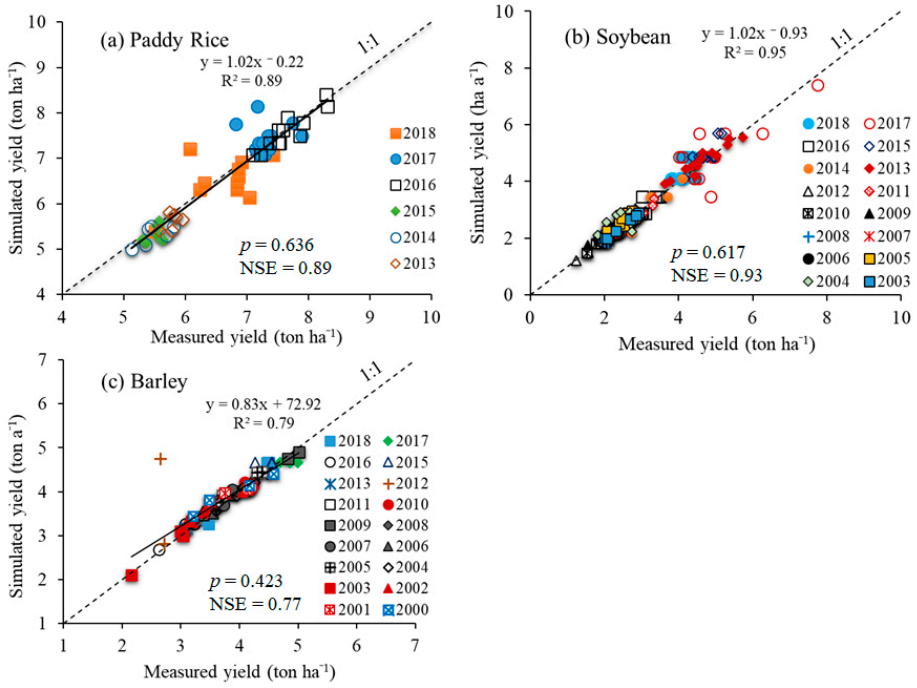

Figure A2. Simulated versus measured yields of rice for six years (**a**), soybean for sixteen years (**b**), and barley for eighteen years (**c**). *p* and NSE represent *p*-values in two-sample *t*-tests and Nash Sutcliffe model efficiency.

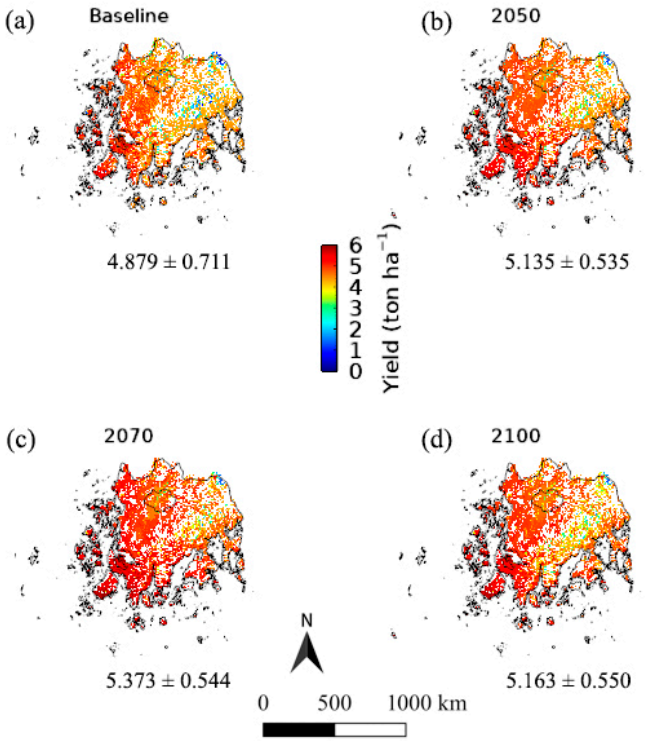

Figure A3. Simulated variations in Ilmi rice yield under the potential climate change impacts of Representative Concentration Pathway 8.5 in 2044–2056 centered on 2050 (**b**), 2064–2076 centered on 2070 (**c**), and 2094–2106 centered on 2100 (**d**) compared to the baseline (**a**) in Chonnam Province, Korea.

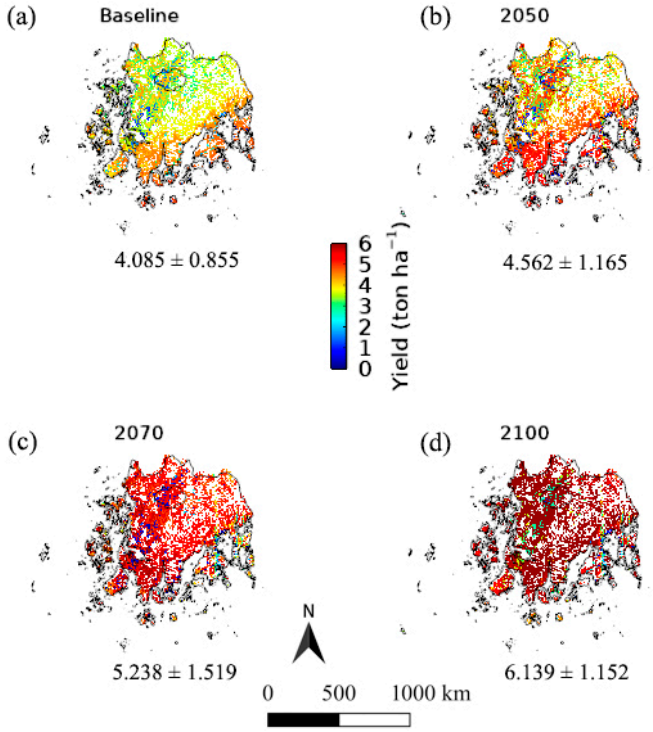

Figure A4. Simulated variations in SaeChal-naked barley yield under the potential climate change impacts of Representative Concentration Pathway 8.5 in 2044–2056 centered on 2050 (**b**), 2064–2076 centered on 2070 (**c**), and 2094–2106 centered on 2100 (**d**) compared to the baseline (**a**) in Chonnam Province, Korea.

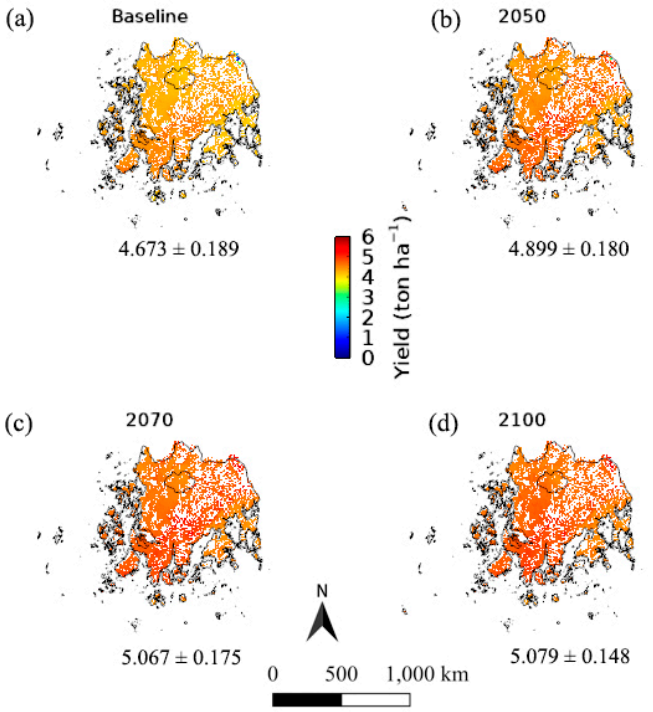

Figure A5. Simulated variations in Daewon soybean yield under the potential climate change impacts of Representative Concentration Pathway 8.5 in 2044–2056 centered on 2050 (**b**), 2064–2076 centered on 2070 (**c**), and 2094–2106 centered on 2100 (**d**) compared to the baseline (**a**) in Chonnam Province, Korea.

References

1. IPCC. Climate Change 2013: The physical science basis. In *Contribution of Working Group I to the Fifth Assessment Report of the Intergovernmental Panel on Climate Change*; Stocker, T.F., Qin, D., Plattner, G.-K., Tignor, M., Allen, P.M., Boschung, J., Nauels, A., Xia, Y., Bex, V., Midgley, P.M., Eds.; Cambridge University Press: Cambridge, UK; New York, NY, USA, 2013.
2. Long, S.P.; Ainsworth, E.A.; Leakey, A.D.; Nösberger, J.; Ort, D.R. Food for thought: Lower-than-expected crop yield stimulation with rising CO_2 concentrations. *Science* **2006**, *312*, 1918–1921. [CrossRef]
3. Rosenzweig, C.; Elliott, J.; Deryng, D.; Ruane, A.C.; Müller, C.; Arneth, A.; Boote, K.J.; Folberth, C.; Glotter, M.; Khabarov, N.; et al. Assessing agricultural risks of climate change in the 21st century in a global gridded crop model intercomparison. *Proc. Natl. Acad. Sci. USA* **2014**, *111*, 3268–3273. [CrossRef]
4. Lobell, D.B.; Burke, M.B.; Tebaldi, C.; Mastrandrea, M.D.; Falcon, W.P.; Naylor, R.L. Prioritizing Climate Change Adaptation Needs for Food Security in 2030. *Science* **2008**, *319*, 607–610. [CrossRef] [PubMed]
5. Ramankutty, N.; Foley, J.A.; Norman, J.; McSweeney, K. The global distribution of cultivable lands: Current patterns and sensitivity to possible climate change. *Glob. Ecol. Biogeogr.* **2002**, *11*, 377–392. [CrossRef]
6. Ko, J.; Tim Ng, C.; Jeong, S.; Kim, J.-H.; Lee, B.; Kim, H.-Y. Impacts of regional climate change on barley yield and its geographical variation in South Korea. *Int. Agrophys.* **2019**, *33*, 81–96. [CrossRef]
7. Lobell, D.B.; Schlenker, W.; Costa-Roberts, J. Climate Trends and Global Crop Production since 1980. *Science* **2011**, *333*, 616–620. [CrossRef] [PubMed]
8. Palosuo, T.; Hoffmann, M.P.; Rötter, R.P.; Lehtonen, H.S. Sustainable intensification of crop production under alternative future changes in climate and technology: The case of the North Savo region. *Agric. Syst.* **2021**, *190*, 103135. [CrossRef]
9. Ko, J.; Kim, H.-Y.; Jeong, S.; An, J.-B.; Choi, G.; Kang, S.; Tenhunen, J. Potential impacts on climate change on paddy rice yield in mountainous highland terrains. *J. Crop Sci. Biotechnol.* **2014**, *17*, 117–126. [CrossRef]
10. Kim, H.Y.; Ko, J.; Kang, S.; Tenhunen, J. Impacts of climate change on paddy rice yield in a temperate climate. *Glob. Chang. Biol.* **2013**, *19*, 548–562. [CrossRef] [PubMed]
11. Ahuja, L.R.; Rojas, K.W.; Hanson, J.D.; Shaffer, M.J.; Ma, L. *Root Zone Water Quality Model: Modeling Management Effects on Water Quality and Crop Production*; Water Resources Publications, LLC.: Highland Ranch, CO, USA, 2000.
12. Kirschbaum, M.U.F. Forest growth and species distribution in a changing climate. *Tree Physiol.* **2000**, *20*, 309–322. [CrossRef] [PubMed]
13. McCown, R.L.; Hammer, G.L.; Hargreaves, J.N.G.; Holzworth, D.P.; Freebairn, D.M. APSIM: A novel software system for model development, model testing and simulation in agricultural systems research. *Agricult. Syst.* **1996**, *50*, 255–271. [CrossRef]
14. Brisson, N.; Gary, C.; Justes, E.; Roche, R.; Mary, B.; Ripoche, D.; Zimmer, D.; Sierra, J.; Bertuzzi, P.; Burger, P.; et al. An overview of the crop model stics. *Eur. J. Agron.* **2003**, *18*, 309–332. [CrossRef]
15. Ma, L.; Hoogenboom, G.; Ahuja, L.; Nielsen, D.; Ascough, J. Development and evaluation of the RZWQM-CROPGRO hybrid model for soybean production. *Agron. J.* **2005**, *97*, 1172–1182. [CrossRef]
16. Williams, J.R. The Erosion-Productivity Impact Calculator (EPIC) Model: A Case History. *Philos. Trans. Biol. Sci.* **1990**, *329*, 421–428.
17. Hijmans, R.J.; Guiking-Lens, I.; Van Diepen, C. *WOFOST 6.0: User's Guide for the WOFOST 6.0 Crop Growth Simulation Model*; DLO Winand Staring Centre: Wageningen, The Netherlands, 1994; p. 145.
18. Jones, J.W.; Hoogenboom, G.; Porter, C.H.; Boote, K.J.; Batchelor, W.D.; Hunt, L.; Wilkens, P.W.; Singh, U.; Gijsman, A.J.; Ritchie, J.T. The DSSAT cropping system model. *Eur. J. Agron.* **2003**, *18*, 235–265. [CrossRef]
19. Singh, U.; Ritchie, J.; Thornton, P. *CERES-Cereal Model for Wheat, Maize, Sorghum, Barley, and Pearl Millet, 1991 Agronomy Abstracts*; ASA: Madison, WI, USA, 1991; p. 78.
20. Boote, K.J.; Jones, J.W.; Hoogenboom, G.; Pickering, N. Simulation of crop growth: CROPGRO model. *Agric. Syst. Modeling Simul.* **1998**, *18*, 651–692.
21. Singh, U.; Matthews, R.B.; Griffin, T.S.; Ritchie, J.T.; Hunt, L.A.; Goenaga, R. Modeling growth and development of root and tuber crops. In *Understanding Options for Agricultural Production*; Tsuji, G.Y., Hoogenboom, G., Thornton, P.K., Eds.; Springer: Dordrecht, The Netherlands, 1998; pp. 129–156. [CrossRef]
22. Kim, H.-Y.; Lim, S.-S.; Kwak, J.-H.; Lee, D.-S.; Lee, S.-M.; Ro, H.-M.; Choi, W.-J. Dry matter and nitrogen accumulation and partitioning in rice (Oryza sativa L.) exposed to experimental warming with elevated CO_2. *Plant Soil* **2011**, *342*, 59–71. [CrossRef]
23. Park, H.-J.; Lim, S.-S.; Kwak, J.-H.; Lee, K.-S.; In Yang, H.; Kim, H.-Y.; Lee, S.-M.; Choi, W.-J. Biomass, chemical composition, and microbial decomposability of rice root and straw produced under co-elevated CO_2 and temperature. *Biol. Fertil. Soils* **2020**, *56*, 991–1005. [CrossRef]
24. Kim, J.; Park, J.; Hyun, S.; Fleisher, D.H.; Kim, K.S. Development of an automated gridded crop growth simulation support system for distributed computing with virtual machines. *Comput. Electron. Agric.* **2020**, *169*, 105196. [CrossRef]
25. Yun, S.-I.; Kang, B.-M.; Lim, S.-S.; Choi, W.-J.; Ko, J.; Yoon, S.; Ro, H.-M.; Kim, H.-Y. Further understanding CH4 emissions from a flooded rice field exposed to experimental warming with elevated [CO_2]. *Agric. For. Meteorol.* **2012**, *154*, 75–83. [CrossRef]
26. Goodin, D.G.; Hutchinson, J.M.S.; Richard, L.V.; Knapp, M.C. Estimating solar irradiance for crop modeling using daily air temperature data. *Agron. J.* **1999**, *91*, 845–851. [CrossRef]
27. Allen, L.H., Jr.; Boote, K.J.; Jones, J.W.; Jones, P.H.; Valle, R.R.; Acock, B.; Rogers, H.H.; Dahlman, R.C. Response of vegetation to rising carbon dioxide: Photosynthesis, biomass, and seed yield of soybean. *Glob. Biogeochem. Cycles* **1987**, *1*, 1–14. [CrossRef]

28. Reyenga, P.J.; Howden, S.M.; Meinke, H.; McKeon, G.M. Modelling global change impacts on wheat cropping in south-east Queensland, Australia. *Environ. Model. Softw.* **1999**, *14*, 297–306. [CrossRef]
29. Jamieson, P.D.; Berntsen, J.; Ewert, F.; Kimball, B.A.; Olesen, J.; Pinter, P.; Porter, J.; Semenov, M. Modelling CO_2 effects on wheat with varying nitrogen supplies. *Agric. Ecosyst. Environ.* **2000**, *82*, 27–37. [CrossRef]
30. Kim, H.-Y.; Ko, J.; Jeong, S.; Kim, J.-H.; Lee, B. Geospatial delineation of South Korea for adjusted barley cultivation under changing climate. *J. Crop Sci. Biotechnol.* **2017**, *20*, 417–427. [CrossRef]
31. Hong, S.Y.; Zhang, Y.-S.; Hyun, B.-K.; Sonn, Y.-K.; Kim, Y.-H.; Jung, S.-J.; Park, C.-W.; Song, K.-C.; Jang, B.-C.; Choe, E.-Y. An introduction of Korean soil information system. *Korea J. Soil Sci. Fert.* **2009**, *42*, 21–28.
32. Ahn, J.; Hur, J.; Shim, K. A simulation of agro-climate index over the Korean peninsula using dynamical downscaling with a numerical weather prediction model. *Korean J. Agric. For. Meteorol.* **2010**, *12*, 1–10. [CrossRef]
33. Ko, J.; Ahuja, L.R.; Saseendran, S.; Green, T.R.; Ma, L.; Nielsen, D.C.; Walthall, C.L. Climate change impacts on dryland cropping systems in the Central Great Plains, USA. *Clim. Chang.* **2012**, *111*, 445–472. [CrossRef]
34. Nash, J.E.; Sutcliffe, J.V. River flow forecasting through conceptual models part I—A discussion of principles. *J. Hydrol.* **1970**, *10*, 282–290. [CrossRef]
35. Ludwig, F.; Asseng, S. Climate change impacts on wheat production in a Mediterranean environment in Western Australia. *Agric. Syst.* **2006**, *90*, 15–179. [CrossRef]
36. Ko, J.; Ahuja, L.; Kimball, B.; Anapalli, S.; Ma, L.; Green, T.R.; Ruane, A.C.; Wall, G.W.; Pinter, P.; Bader, D.A. Simulation of free air CO_2 enriched wheat growth and interactions with water, nitrogen, and temperature. *Agric. For. Meteorol.* **2010**, *150*, 1331–1346. [CrossRef]
37. Fu, T.; Ha, B.; Ko, J. Simulation of CO_2 enrichment and climate change impacts on soybean production. *Int. Agrophys.* **2016**, *30*, 25–37. [CrossRef]
38. Lobell, D.B.; Field, C.B. Global scale climate–crop yield relationships and the impacts of recent warming. *Environ. Res. Lett.* **2007**, *2*, 014002. [CrossRef]
39. Elliott, J.; Müller, C.; Deryng, D.; Chryssanthacopoulos, J.; Boote, K.J.; Büchner, M.; Foster, I.; Glotter, M.; Heinke, J.; Iizumi, T.; et al. The Global Gridded Crop Model Intercomparison: Data and modeling protocols for Phase 1 (v1.0). *Geosci. Model Dev.* **2015**, *8*, 261–277. [CrossRef]
40. Gornall, J.; Betts, R.; Burke, E.; Clark, R.; Camp, J.; Willett, K.; Wiltshire, A. Implications of climate change for agricultural productivity in the early twenty-first century. *Philos. Trans. R. Soc. B Biol. Sci.* **2010**, *365*, 2973–2989. [CrossRef] [PubMed]
41. Olesen, J.E.; Trnka, M.; Kersebaum, K.C.; Skjelvåg, A.O.; Seguin, B.; Peltonen-Sainio, P.; Rossi, F.; Kozyra, J.; Micale, F. Impacts and adaptation of European crop production systems to climate change. *Eur. J. Agron.* **2011**, *34*, 96–112. [CrossRef]
42. Li, S.; Wang, Q.; Chun, J.A. Impact assessment of climate change on rice productivity in the Indochinese Peninsula using a regional-scale crop model. *Int. J. Climatol.* **2017**, *37*, 1147–1160. [CrossRef]
43. Thornton, P.K.; Jones, P.G.; Alagarswamy, G.; Andresen, J. Spatial variation of crop yield response to climate change in East Africa. *Glob. Environ. Chang.* **2009**, *19*, 54–65. [CrossRef]
44. Adams, R.M.; Rosenzweig, C.; Peart, R.M.; Ritchie, J.T.; McCarl, B.A.; Glyer, J.D.; Curry, R.B.; Jones, J.W.; Boote, K.J.; Allen, L.H. Global climate change and US agriculture. *Nature* **1990**, *345*, 219–224. [CrossRef]
45. Lee, J.; De Gryze, S.; Six, J. Effect of climate change on field crop production in California's Central Valley. *Clim. Chang.* **2011**, *109*, 335–353. [CrossRef]
46. Hatfield, J.L.; Boote, K.J.; Kimball, B.A.; Ziska, L.; Izaurralde, R.C.; Ort, D.; Thomson, A.M.; Wolfe, D. Climate Impacts on Agriculture: Implications for Crop Production. *Agron. J.* **2011**, *103*, 351–370. [CrossRef]
47. Lövenstein, H.; Rabbinge, R.; van Keulen, H. *World Food Production, Textbook 2: Biophysical Factors in Agricultural Production*; Wageningen University & Research: Wageningen, The Netherlands, 1992.